NANO LETTERS

Letter

pubs.acs.org/NanoLett

Self-Folding Single Cell Grippers

Kate Malachowski,[†] Mustapha Jamal,[†] Qianru Jin,[†] Beril Polat,[†] Christopher J. Morris,[‡] and David H. Gracias*[,†]

[†]Department of Chemical and Biomolecular Engineering, The Johns Hopkins University, 3400 N. Charles St., Baltimore, Maryland 21218, United States

[‡]United States Army Research Laboratory, Sensors and Electron Devices Directorate, 2800 Powder Mill Rd., Adelphi, Maryland 20783, United States

Supporting Information

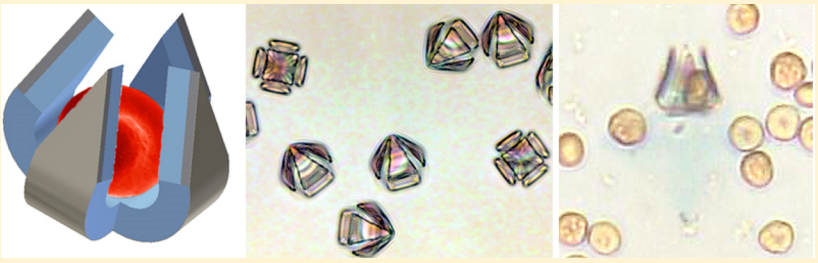

ABSTRACT: Given the heterogeneous nature of cultures, tumors, and tissues, the ability to capture, contain, and analyze single cells is important for genomics, proteomics, diagnostics, therapeutics, and surgery. Moreover, for surgical applications in small conduits in the body such as in the cardiovascular system, there is a need for tiny tools that approach the size of the single red blood cells that traverse the blood vessels and capillaries. We describe the fabrication of arrayed or untethered single cell grippers composed of biocompatible and bioresorbable silicon monoxide and silicon dioxide. The energy required to actuate these grippers is derived from the release of residual stress in 3−27 nm thick films, did not require any wires, tethers, or batteries, and resulted in folding angles over 100° with folding radii as small as 765 nm. We developed and applied a finite element model to predict these folding angles. Finally, we demonstrated the capture of live mouse fibroblast cells in an array of grippers and individual red blood cells in untethered grippers which could be released from the substrate to illustrate the potential utility for in vivo operations.

KEYWORDS: *Self-assembly, origami, lab-on-a-chip, surgery, nanomedicine, nanomechanics, robotics*

Because of the large size of tools that are typically utilized for surgical diagnostics and biological analyses, cellular samples are often large in size. Consequently, the data collected from tissue biopsied samples and related assays average over a multitude of cells. However, that average may not accurately represent the behavior of individual cells, particularly if the cells of interest are a small fraction of the population. Further, it can be challenging to draw conclusions about dynamic or transient behaviors of single cells by looking at large populations.[1−3] Tumors have long been known to be heterogeneous populations of cells with varying phenotypes and genotypes, proliferation rate, potential for metastasis, and drug responsiveness, yet we are only beginning to understand how these heterogeneities affect their progression.[4−7] Single cell analyses may be necessary to differentiate the behavior of a cell subpopulation from the bulk sample, particularly in the fields of cancer biology, genomics, proteomics, stem cell biology, and hematology.[3] This work is especially important as treatments for cancer, immune diseases, and tissue regeneration move toward personalized medicine.[8]

A wide range of techniques are available for in vitro single cell analysis, and each has advantages and disadvantages in terms of efficiency, cell manipulation, imaging capability, sensitivity, and ability to mimic or actually perform in vivo.[9,10] These methods include flow cytometry,[9] optical traps,[11−16] microfluidic traps and devices,[2,17−26] microwells,[27,28] microtubes,[29] and 2D surface patterns.[30−34] Several miniaturized robotic devices have been created to trap and manipulate particles and cells with precise control.[35−37] For example, Chronis et al. demonstrate the manipulation of a 10 μm cell using a wired, electrothermally actuated SU-8 gripper.[35] This device can manipulate cells with high precision, but the electrical wires that control its actuation and its large back-end design limit throughput and in vivo utility. Another SU-8 device, by Sakar et al., provides untethered manipulation of single cells via magnetic forces with minimal fluid disturbance due to its micrometer size and biocompatibility.[36] However, these devices are passive, trapping cells in a recess, and thus they may lose their grip on a cell if moved in the wrong direction or in all three dimensions. A significant hurdle in the

Received: May 19, 2014
Revised: June 5, 2014
Published: June 10, 2014

   dx.doi.org/10.1021/nl500136a | *Nano Lett.* 2014, 14, 4164−4170

creation of active single cell devices with moving parts is the challenge in harnessing energy at small size scales and in a highly parallel and untethered manner.

An ideal in vitro device would combine the high throughput efficiency of flow cytometry, the incorporation of patterned microfeatures for biomolecular analyses, and the 3D manipulation precision of optical tweezers. An ideal in vivo device should be composed of biocompatible and possibly bioresorbable materials while facilitating tissue excision or targeted capture, robust gripping, and retrieval in an autonomous manner.[38] Here, we describe an important step toward achieving tools that combine both of these in vitro and in vivo capabilities for single cell studies and to potentially access tiny conduits in the body. Our approach is inspired by previous studies on the stress-based roll-up and self-folding of thin films and the energy required to enable gripper motion is derived from the differential residual stress in nanoscale bilayers.[39−64] The approach utilizes photolithography, which is a high throughput technique capable of fabricating 500 000 to 10 million single grippers on a 3 in. wafer or potentially over 100 million on a 12 in. wafer which is the size of wafers used currently in CMOS fabrication facilities. Additionally, the grippers can be actuated to close around single cells en masse, creating devices with patterns in all three dimensions. The thickness of the films can be varied to control the fold angle, while the sharpness of the tips could aid with the capture and containment of cells. As compared to previously described stimuli responsive "μ-grippers" that were used to biopsy cell samples and porcine organs under in vitro, ex vivo, and in vivo conditions,[54,65−67] these grippers are 30 times smaller, requiring significantly thinner hinges and different materials to achieve a tight radius of curvature. While we previously utilized the larger μ-grippers only in the gastrointestinal (GI) tract, we envision that these single cell sized grippers could be used in tighter spaces such as within the circulatory, urinogenital, or central nervous system. In these regions, however, there are more stringent requirements on biocompatibility and biodegradability for these applications.[38]

In light of the more stringent biodegradability requirements and the need for small devices, considerable thought was given to the materials chosen for these single cell grippers. Silicon (Si) and silicon dioxide (SiO_2) react with water via hydrolysis to form $Si(OH)_4$[68,69] and thus dissolve into DI water and various biofluids[68,70] as previously reported by Hwang et al. in their work on transient electronics.[70] Additionally, electronic devices made from Si, SiO_2, and other metals were implanted subdermally into mice with no significant inflammatory reactions and almost complete dissolution in 3 weeks. Silicon monoxide (SiO) is a two-phase, nonhomogenous mixture of amorphous Si and SiO_2 and has been previously paired with SiO_2 to form tightly rolled tubes with microscale radii of curvature when deposited by electron beam (e-beam) evaporation in nanometer-scale thicknesses.[29,52,59,60,76,77] Thus, we selected these two silicon-based oxides for our single cell grippers for their biocompatibility, bioresorbability, and self-curling properties. We independently verified the dissolution of SiO and SiO_2 in phosphate-buffered saline solution (PBS) over a 20 day period at 37 °C. Thirty nanometer films of SiO_2 dissolved at a rate of 2 nm/day at 37 °C, while SiO dissolved more slowly at less than 1 nm/day (Figure S1).

Grippers were fabricated with flexible, prestressed bilayer hinges, connected to rigid segments (Figure 1a). The prestressed bilayer was constructed from e-beam evaporated thin films of SiO and SiO_2. The rigid segments were formed from thicker films of e-beam evaporated SiO. A stimuli-responsive hinge trigger could be patterned or molded atop the grippers to control actuation.[54,65−67,71] These devices can either be arrayed on a substrate for use as a single cell in vitro analytical assay device or completely released to be used as free-floating or untethered tools (Figure 1b−c). Detailed thicknesses and evaporation conditions are in the Suppporting Information (Table S1).

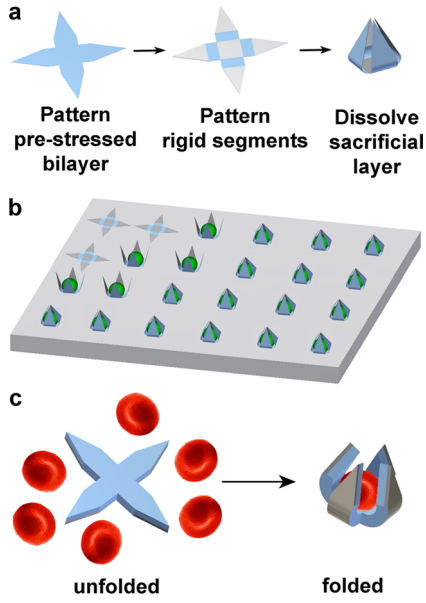

Figure 1. Illustration of single cell gripper fabrication and use on substrates or as untethered tools. (a) Fabrication scheme for creating single cell grippers. The prestressed actuator hinge is a SiO/SiO_2 bilayer, while the rigid segments are made of SiO. Upon dissolution of the sacrificial layer, the arms are released and self-actuate to close around cells. An optional thermoresponsive trigger layer can be molded atop the grippers. (b) Illustration of cells captured by single cell microgrippers arrays. (c) Illustration of untethered single cell grippers and red blood cell capture.

We developed several gripper variants with three or four arms, varying in size from 10 to 70 μm in length (tip-to-tip when open), which is an appropriate size range to grasp a variety of individual cells (Figure 2a). The alternating rigid frames and flexible hinges are evident in the open grippers (Figure 2b, d). Grippers folded at angles ranging from 90° to 115° depending on the bilayer film thickness, corresponding to folding radii ranging from to 765 nm to 5 μm. The film thickness could be adjusted to assemble tightly folded grippers in a range of sizes. For example, 9 nm of SiO and 27 nm of SiO_2 were deposited to assemble the 50 μm grippers shown in Figure 2b and c, while a bilayer of 3 nm of SiO and 3 nm of SiO_2 was used to assemble the 10 μm grippers in Figure 2d and e. Despite their small sizes, these grippers were fabricated using photolithography on a projection mask aligner with 500 nm resolution. Photolithography and registry of multiple film layers became increasingly difficult as the size of the grippers decreased for the specific tools used, leading to a lower limit for an open tip to tip gripper size of about 10 μm. In principle, smaller grippers could be fabricated using serial e-beam lithography, but quantities would be limited due to the serial nature of that technique, and the sizes would be smaller than those of single cells thereby limiting use.

dx.doi.org/10.1021/nl500136a | Nano Lett. 2014, 14, 4164−4170

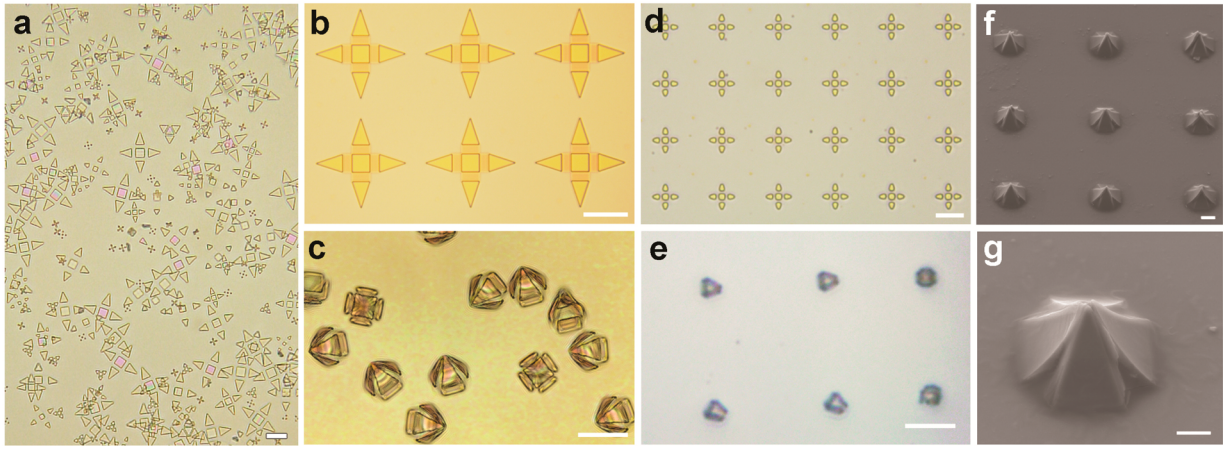

Figure 2. Optical images of single cell grippers before and after closing. (a) Optical image of grippers released from the substrate with open arms prior to closing, in sizes ranging from 10 to 50 μm. (b–c) Zoomed optical images of 50 μm grippers (b) prior to release from the substrate and (c) closed tightly after release. (d–e) Optical images of 10 μm grippers (d) open and (e) closed. Scale bars are (a, b, c) 25 μm and (d, e) 10 μm. (f–g) SEM images at different magnifications of closed single cell grippers attached to the substrate. Scale bars are (f) 10 μm and (g) 5 μm.

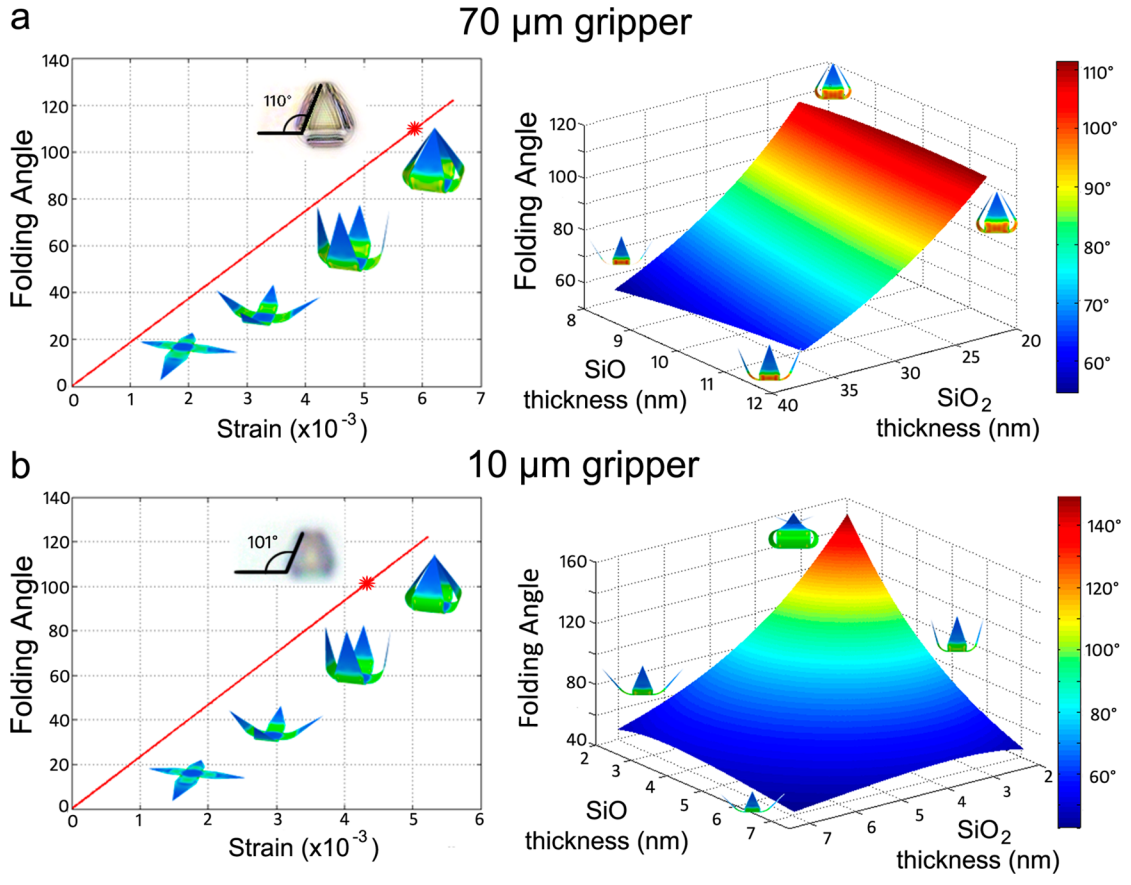

Figure 3. Characterization of thin film stress and gripper folding angle. (a) Graphs depicting the effect of mismatch strain (left panel) and SiO/SiO_2 thickness (right panel) on folding angle for the 70 μm gripper. (b) Graphs depicting the effect of mismatch strain (left panel) and SiO/SiO_2 thickness (right panel) on folding angle for the 10 μm gripper. The inset images of a folded gripper with angle measurement in the left panels are optical microscopy images of actual folded grippers for comparison to the modeled gripper folding. The red star on these graphs indicates the experimentally observed folding angle for these experimentally observed grippers. More details of the parameters used to generate the models and graphs are in the Supporting Information.

The radius of curvature of each gripper hinge is related to the film thickness, mechanical properties of the materials, and residual stress of each layer within the prestressed bilayer. It is noteworthy that previous designs of μ-grippers were made from either a chromium/copper (Cr/Cu) bilayer or a chromium/gold (Cr/Au) bilayer.[54,66,67] In those designs, the Cr layer had significant tensile stress (~1 GPa), while the Cu or Au layer was relatively neutral in stress. This stress differential caused the grippers to fold due to the shared boundary between the two layers. These previously utilized metallic combinations,

dx.doi.org/10.1021/nl500136a | Nano Lett. 2014, 14, 4164–4170

however, were unable to curl with a radius of curvature less than about 30 μm, limiting a multisegmented gripper device to larger than 200 μm in tip to tip size when open. However, as we describe in this work, the SiO/SiO_2 combination provided a sufficiently small radius of curvature for single cell grippers, with radii as small as 765 nm.

We characterized the residual stress within the SiO and SiO_2 films. We found the stress in both SiO and SiO_2 to be compressive, with less compressive stress as thicknesses increased from 10 to 100 nm (Figure S2a). These stress values varied significantly with thicknesses below 100 nm but were consistent with the expected range of compressive stress for the deposition conditions used.[72,73] However, a more important parameter for SiO_2 film stress was the time of exposure to room air following deposition in an evaporation chamber. We observed an increasing tensile component in SiO_2 films over time (Figure S2b), while the stress in SiO films remained generally constant. We attribute the change in SiO_2 stress to the absorption of water by SiO_2, and the subsequent reaction between water and dangling Si bonds that leads to a tensile stress component that grows linearly with the logarithm of aging time.[74] By using SiO_2 films to form the inside of each concave folded hinge, we ensured that the growth of this tensile stress component helped each hinge fold with a sufficiently small radius of curvature.

We examined the effect of preload strain and film thickness on the folding angle using an analytical curvature model[75] and a computational finite element analysis (FEA) simulation (Figure 3 and Figures S3–S5). Details of the models are given in the Supporting Information. We modeled the effect of strain on folding angle for a 70 μm and a 10 μm gripper (Figure 3) and found that as the strain increased the folding angle also increased which is expected. Larger mismatch strain allows the gripper to fold more tightly. One can tune the strain by choosing different materials and adjusting thin film deposition condition. Film thickness is also a tunable property in gripper fabrication and greatly affects the folding angle. We performed a thickness sensitivity analysis by modeling the folding angle versus SiO and SiO_2 film thickness for a 70 μm and a 10 μm gripper. In general, due to larger bending stiffness, the folding angle decreases as film thickness increases; thus for the smallest grippers, films on the order of 3–5 nm were required. However, grippers with films that are too thin may be too fragile for use in real biological applications. These plots, and other detailed plots given in the Supporting Information, serve as design guides for determining the necessary thicknesses for each layer within the prestressed bilayer to achieve a desired folding angle.

One application we envision for these devices is an in vitro arrayed analytical device that could be used to entrap many single cells for biological assays. As these devices can be patterned in all three dimensions and grip en masse, many individual cells can be trapped, assayed, and imaged with a high yield. To demonstrate this application, we fabricated 50 μm grippers that remain attached to the substrate upon release of the arms. The arms were patterned on a Cu sacrificial layer and were thus able to fold. The center or "base" of the gripper was patterned directly onto the Si wafer so that it remained attached during the release and folding process. We pipetted live L-929 mouse fibroblasts in media on top of the open grippers. The grippers closed around individual cells after 2–6 h in warm culture media due to the slow etching action of the ions in the media (Figure 4). Thus, in this application, no hinge trigger is required as cells are captured during the release of the gripper arms from the substrate. The gripper arms closed around each cell, and the cells remained viable as evidenced by the green fluorescence of the cell bodies from the calcein stain of the live/dead assay. Some grippers were empty, but when occupied, each of the grippers contained only one cell. Our best observed yield for successfully filled grippers was 48% for an area of approximately 75 grippers. The concentration of cells used in the suspension significantly impacted the yield of capture. The optimal concentration created a single layer of well-distributed cells, wherein each gripper was touching at least one cell. This optimal concentration varied with the size of the grippers. The SiO/SiO_2 grippers also are optically transparent and thus are ideal for imaging the entrapped cells using optical microscopy techniques. These grippers have slit openings at the intersection of the arms, and consequently, nutrients, waste, and other biochemicals can flow easily to and from the cells, yet

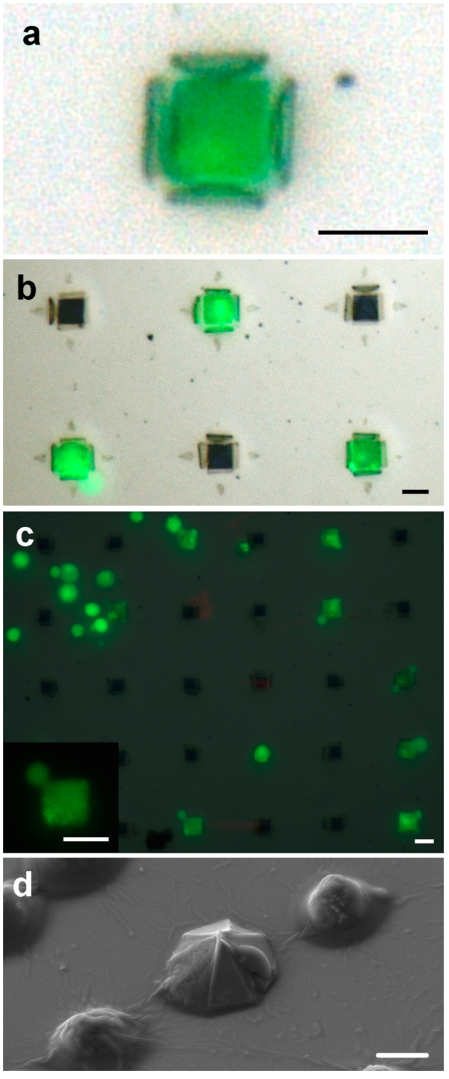

Figure 4. Single cell microgripper arrays. (a–c) Individual cells captured within the arms of grippers. Since the films are optically transparent, cells captured by the grippers can be readily visualized using optical microscopy. (c, inset) The cell shown is entrapped by a gripper, as evidenced by the square appearance of the cell when viewed from the top, which matches the square shape of the base of the gripper. (d) SEM image of a cell trapped within the arms of a gripper, surrounded by untrapped cells. Scale bars are 10 μm.

dx.doi.org/10.1021/nl500136a | *Nano Lett.* 2014, 14, 4164–4170

we observed that the grippers held all cells in place during staining and imaging. We performed a live/dead assay by staining with calcein AM and ethidium homodimer after the cells were captured (Figure 4a–c). The cells fluoresced green, demonstrating that they are alive, and that the assay chemicals successfully diffused between the grippers arms. Thus, the grippers did not kill the cells, and they allow the cells access to any chemicals within the media.

To verify that the cells were in fact contained inside the grippers, we fixed the cells and performed scanning electron microscopy (SEM) on an array of grippers with isolated fixed cells (Figure 4d). This image confirms that the cell was contained within the arms of the gripper, as opposed to floating on top of the gripper. It is noteworthy that the cells conformed to the shape of the gripper, as evidenced both in the SEM and by the square shape of the green fluorescing cells (Figure 4c inset, 4d), highlighting potential interactions with the faces of the gripper.

We also investigated applicability of grippers to capture red blood cells from a beagle blood sample (Figure 5). While the previous experiment captured L-929 fibroblasts and remained anchored to the substrate for further analysis, here we release the grippers from the substrate to show the potential for cells to be captured and moved in solution. We chose a 35 μm open gripper size which is about 4–5 times the size of the red blood cells (6–8 μm in size). The central palm of these grippers is matched to the size of the red blood cells ensuring that the cells could be entrapped within the gripper in a snug fit. Initially, red blood cells were pipetted onto partially released grippers. Many grippers were able to trap single blood cells within their arms.

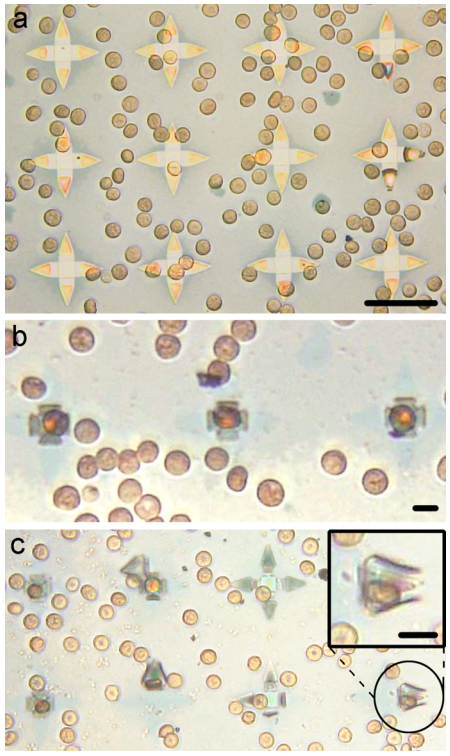

Figure 5. Capture of single red blood cells and untethered single cell grippers. (a–c) Optical images of red blood cells trapped in 35 μm SiO/SiO_2 grippers. (a) Grippers with red blood cells prior to folding and release from the substrate. Scale bar is 35 μm. (b–c) Red blood cells captured by the grippers. Scale bars are 10 μm.

Optical profilometry and microscopy of the grippers confirmed that the cells were trapped within the grippers. This experiment highlights the potential for these devices as in vivo cell capture tools. This application would require a biocompatible, thermo- or chemo-responsive hinge trigger, as previously demonstrated on larger grippers.[54,65−67,71] Whereas these larger grippers were able to capture large clumps of tissue in vivo, the single cell grippers could potentially enable the capture of individual cells.

We noted previously that both SiO and SiO_2 dissolve over time in biological fluids; therefore, grippers composed of such materials have significant potential for both in vitro and in vivo applications. Since the dissolution rate of these materials in bodily fluids is known to be dependent on a number of parameters such as method of thin film deposition, thickness, pH, and volume of fluid, further studies will be needed to design and optimize bioresorbability and safety for specific surgical applications in different biological environments in vivo.[78,79] For example, given the faster rate of dissolution of SiO_2 in PBS, grippers designed for in vivo use could be fabricated with SiO_2 rigid segments for rapid elimination from the body. Grippers fabricated with SiO rigid segments, like those shown in these figures, are best suited to in vitro applications for biocompatibility and slow degradation. If needed, such tools could also be created with magnetic elements using highly stressed bilayers of nickel (Ni) with rigid Ni panels for guidance through narrow conduits using magnetic fields (Figure S6). As an additional form of motion control, patterned biomarkers on the grippers could enable targeting of specific diseased cells in vivo.

In summary, we have designed and fabricated grippers capable of capturing and isolating single cells. These single cell grippers, made from biocompatible, optically transparent materials, can be arrayed for high throughput in vitro assays and imaging or released for use as untethered tools. We employed varying sizes of these grippers to capture individual fibroblasts and red blood cells. These cells were alive and could be assayed or fixed for imaging. Because these devices are fabricated in 2D and subsequently folded into 3D, future studies could explore patterned topography such as spikes, holes, nanoscale roughness, and biochemical surface functionalizations in specific designs onto one or more device walls. This approach could enable multiple assays to be run at one time on a single cell. Additionally, our group has previously demonstrated the fabrication of many differently shaped polyhedra.[51,80] Future studies could utilize pyramidal grippers and other regular polyhedra to study the effect of 3D confinement on cell growth and morphology. Our process is amenable to other lithographic approaches such as e-beam or nanoimprint lithography for subcellular gripping capabilities. Finally, this work highlights the potential for the creation of untethered active single cell capture devices. When doped with magnetic elements or made from magnetic materials such as nickel, these devices could be guided using magnetic fields[36,54,65−67,81] and consequently used as in vitro single cell capture devices as an alternative to laser microdissection of tissue samples. Due to their small size, they could also be utilized as bioresorbable surgical tools and in vivo single cell capture devices that are able to traverse conduits within the circulatory, central nervous, and urogenital systems.

dx.doi.org/10.1021/nl500136a | *Nano Lett.* 2014, 14, 4164–4170

■ ASSOCIATED CONTENT

Supporting Information

Thin film stress and folding characterization. This material is available free of charge via the Internet at http://pubs.acs.org.

■ AUTHOR INFORMATION

Corresponding Author

*E-mail: dgracias@jhu.edu.

Author Contributions

M.J. and Q.J. contributed equally. D.H.G. and K.M. conceived of these devices and designed the experiments. K.M. conducted all experiments. M.J. performed SEM microscopy and optical microscopy for Figures 2 and 4 and consulted on fabrication strategies and cell experiments. Q.J. conducted finite element analysis modeling and performed the SiO/SiO_2 dissolution study. B.P. aided with red blood cell experiments and assembly of supplemental figures. C.J.M. performed stress analyses and consulted on modeling. D.H.G., K.M., and Q.J. wrote the paper. All authors commented on and/or edited the manuscript and figures.

Notes

The authors declare no competing financial interest.

■ ACKNOWLEDGMENTS

This research was supported by NIH 1DP2OD004346 and the National Science Foundation grants CBET-1066898 and CMMI-1200241, the Army Research Laboratory, and Northrop Grumman. We thank Professor Benjamin Schaffer for assistance with the modeling software.

■ REFERENCES

(1) Altschuler, S. J.; Wu, L. F. *Cell* **2010**, *141*, 559−563.
(2) Ma, C.; Fan, R.; Admad, H.; Shi, Q.; Comin-Anduix, B.; Chodon, T.; Koya, R. C.; Liu, C.-C.; Kwong, G. A.; Radu, C. G.; Ribas, A.; Heath, J. R. *Nat. Med.* **2011**, *17*, 738−743.
(3) Di Carlo, D.; Tse, H. T. K.; Gossett, D. R. Introduction: Why Analyze Single Cells? In *Single-Cell Analysis: Methods and Protocols*; Lindstrom, S., Andersson-Svahn, H., Eds.; Springer Science + Business Media: New York, 2012; Vol. *853*.
(4) Navin, N.; Krasnitz, A.; Rodgers, L.; Cook, K.; Meth, J.; Kendall, J.; Riggs, M.; Eberling, Y.; Troge, J.; Grubor, V.; Levy, D.; Lundin, P.; Maner, S.; Zetterberg, A.; Hicks, J.; Wigler, M. *Genome Res.* **2010**, 68−80.
(5) Calbo, J.; van Montfort, E.; Proost, N.; van Drunen, E.; Beverloo, H. B.; Meuwissen, R.; Berns, A. *Cancer Cell* **2011**, *19*, 244−256.
(6) Pietras, A. *Adv. Cancer Res.* **2011**, *112*, 255−281.
(7) Mannello, F. *BMC Med.* **2013**, *11*, 169−173.
(8) Beckman, R. A.; Schemmann, G. S.; Yeang, C.-H. *Proc. Natl. Acad. Sci. U.S.A.* **2012**, *109*, 14586−14591.
(9) Lindström, S.; Andersson-Svahn, H. *Lab Chip* **2010**, *10*, 3363−3372.
(10) Lindström, S.; Andersson-Svahn, H. *Single Cell Analysis: Methods and Protocols*; Springer Science + Business Media: New York, 2012; Vol. *853*.
(11) Ashkin, A.; Dziedzic, J. M.; Bjorkholm, J. E.; Chu, S. *Opt. Lett.* **1986**, *11*, 288−290.
(12) Townes-Anderson, E.; St. Jules, R. S.; Sherry, D.; Lichtenberger, J.; Hassanain, M. *Mol. Vision* **1998**, *4*, 12.
(13) Berns, M. W.; Tadir, Y.; Liang, H.; Tromberg, B. *Methods Cell Biol.* **1998**, *55*, 71−98.
(14) Xie, C.; Dinno, M. A.; Li, Y.-q. *Opt. Lett.* **2002**, *27*, 249−251.
(15) Lúcio, A.; Santos, R.; Mesquita, O. *Phys. Rev. E* **2003**, *68*, 041906.
(16) Zhang, H.; Liu, K.-K. *J. R. Soc. Interface* **2008**, *5*, 671−690.
(17) Wheeler, A. R.; Throndset, W. R.; Whelan, R. J.; Leach, A. M.; Zare, R. N.; Liao, Y. H.; Farrell, K.; Manger, I. D.; Daridon, A. *Anal. Chem.* **2003**, *75*, 3581−3586.
(18) Peng, X.; Li, P. *Anal. Chem.* **2004**, *76*, 5273−5281.
(19) Peng, X.; Li, P. *Anal. Chem.* **2004**, *76*, 5282−5292.
(20) Valero, A.; Merino, F.; Wolbers, F.; Luttge, R.; Vermes, I.; Andersson, H.; van den Berg, A. *Lab Chip* **2005**, *5*, 49−55.
(21) Di Carlo, D.; Wu, L. Y.; Lee, L. *Lab Chip* **2006**, *6*, 1445−1449.
(22) Di Carlo, D.; Aghdam, N.; Lee, L. *Anal. Chem.* **2006**, *78*, 4925−4930.
(23) Roman, G. T.; Chen, Y.; Viberg, P.; Culbertson, A. H.; Culbertson, C. T. *Anal. Bioanal. Chem.* **2007**, *387*, 9−12.
(24) Nilsson, J.; Evander, M.; Hammarström, B.; Laurell, T. *Anal. Chim. Acta* **2009**, *649*, 141−157.
(25) Park, S.; Zhang, Y.; Wang, T. H.; Yang, S. *Lab Chip* **2011**, *11*, 2893−2900.
(26) Ding, X.; Lin, S.-C. S.; Kiraly, B.; Yue, H.; Li, S.; Chiang, I.-K.; Shi, J.; Benkovic, S. J.; Huang, T. J. *Proc. Natl. Acad. Sci. U.S.A.* **2012**, *109*, 11105−11109.
(27) Charnley, M.; Textor, M.; Khademhosseini, A.; Lutolf, M. *Integr. Biol.* **2009**, *1*, 625−634.
(28) Lindström, S.; Andersson-Svahn, H. *Biochim. Biophys. Acta* **2011**, *1810*, 308−316.
(29) Smith, E. J.; Xi, W.; Makarov, D.; Monch, I.; Harazim, S. M.; Bolanos Quinones, V. A.; Schmidt, C. K.; Mei, Y.; Sanchez, S.; Schmidt, O. G. *Lab Chip* **2012**, *12*, 1917−1931.
(30) Kane, R. S.; Takayama, S.; Ostuni, E.; Ingber, D. E.; Whitesides, G. M. *Biomaterials* **1999**, *20*, 2363−2376.
(31) Azioune, A.; Storch, M.; Bornens, M.; Thery, M.; Piel, M. *Lab Chip* **2009**, *9*, 1640−1642.
(32) Gautrot, J. E.; Trappmann, B.; Oceguera-Yanez, F.; Connelly, J.; He, X.; Watt, F. M.; Huck, W. T. S. *Biomaterials* **2010**, *31*, 5030−5041.
(33) Leclair, A. M.; Ferguson, S. S. G.; Lagugne-Labathet, F. *Biomaterials* **2011**, *32*, 1351−1360.
(34) Mandal, K.; Balland, M.; Bureau, L. *PLoS One* **2012**, *7*, e37548.
(35) Chronis, N.; Lee, L. P. *J. Microelectromech. Syst.* **2005**, *14*, 857−863.
(36) Sakar, M. S.; Steager, E. B.; Kim, D. H.; Kim, M. J.; Pappas, G. J.; Kumar, V. *Appl. Phys. Lett.* **2010**, *96*, 043705.
(37) Kim, S.; Qiu, F.; Kim, S.; Ghanbari, A.; Moon, C.; Zhang, L.; Nelson, B.; Choi, H. *Adv. Mater.* **2013**, *25*, 5863−5868.
(38) Fernandes, R.; Gracias, D. H. *Mater. Today* **2009**, *12*, 14−20.
(39) Prinz, V. Y.; Seleznev, V. A.; Gutakovsky, A. K.; Chehovskiy, A. V.; Preobrazhenskii, V. V.; Putyato, M. A.; Gavrilova, T. A. *Phys. E (Amsterdam, Neth.)* **2000**, *6*, 828−831.
(40) Schmidt, O. G.; Eberl, K. *Nature* **2001**, *410*, 168.
(41) Kazuyoshi, K.; Fleischmann, T.; Saravanan, S.; Vaccaro, P. O.; Aida, T. *Jpn. J. Appl. Phys.* **2003**, *42*, 4079−4083.
(42) Chua, C. L.; Fork, D. K.; van Schuylenbergh, K.; Lu, J.-P. *J. Microelectromech. Syst.* **2003**, *12*, 989−995.
(43) Prinz, V. Y. *Russ. Phys. J.* **2003**, *46*, 568−576.
(44) Zhanga, L.; Goloda, S. V.; Deckardta, E.; Prinz, V. Y.; Grützmachera, D. *Phys. E (Amsterdam, Neth.)* **2004**, *23*, 280−284.
(45) Sasaki, M.; Briand, D.; Noell, W.; de Rooij, N. F. *IEEE J. Sel. Top. Quantum Electron.* **2004**, *10*, 455−461.
(46) Huang, M.; Boone, C.; Roberts, M.; Savage, D. E.; Lagally, M. G.; Shaji, N.; Qin, H.; Naim, J. A.; Liu, F. *Adv. Mater.* **2005**, *17*, 2860−2864.
(47) Arora, W. J.; Nichol, A. J.; Smith, H. I.; Barbastathis, G. *Appl. Phys. Lett.* **2006**, *88*, 053108.
(48) Moiseeva, E.; Senousy, Y. M.; Harnett, C. K. *J. Micromech. Microeng.* **2007**, *17*, N63−N68.
(49) Stellman, P.; Buchner, T.; Arora, W. J.; Barbastathis, G. *J. Microelectromech. Syst.* **2007**, *16*, 932−949.
(50) Bassik, N.; Stern, G. M.; Jamal, M.; Gracias, D. H. *Adv. Mater.* **2008**, *20*, 4760−4764.
(51) Leong, T. G.; Benson, B. R.; Call, E. K.; Gracias, D. H. *Small* **2008**, *4*, 1605−1609.

(52) Mei, Y.; Huang, G.; Solovev, A. A.; Bermudez Urena, E.; Monch, I.; Ding, F.; Reindl, T.; Fu, R. K. Y.; Chu, P. K.; Schmidt, O. G. *Adv. Mater.* **2008**, *20*, 4085−4090.
(53) Solovev, A. A.; Mei, Y.; Ureña, E. B.; Huang, G.; Schmidt, O. G. *Small* **2009**, *5*, 1688−1692.
(54) Leong, T. G.; Randall, C. L.; Benson, B. R.; Bassik, N.; Stern, G. M.; Gracias, D. H. *Proc. Natl. Acad. Sci. U.S.A.* **2009**, *106*, 703−708.
(55) Huang, G.; Mei, Y.; Thurmer, D. J.; Coric, E.; Schmidt, O. G. *Lab Chip* **2009**, *9*, 263−268.
(56) Bassik, N.; Stern, G. M.; Gracias, D. H. *Appl. Phys. Lett.* **2009**, *95*, 091901.
(57) Mei, Y.; Thurmer, D. J.; Deneke, C.; Kiravittaya, S.; Chen, Y.-F.; Dadgar, A.; Bertram, F.; Bastek, B.; Krost, A.; Christen, J.; Reindl, T.; Stoffel, M.; Coric, E.; Schmidt, O. G. *ACS Nano* **2009**, *3*, 1663−1668.
(58) Jamal, M.; Bassik, N.; Cho, J.-H.; Randall, C. L.; Gracias, D. H. *Biomaterials* **2010**, *31*, 1683−1690.
(59) Shenoy, V. B.; Gracias, D. H. *MRS Bull.* **2012**, *37*, 847−854.
(60) Harazim, S. M.; Xi, W.; Schmidt, C. K.; Sanchez, S.; Schmidt, O. G. *J. Mater. Chem.* **2012**, *22*, 2878−2884.
(61) Xi, W.; Solovev, A. A.; Ananth, A. N.; Gracias, D. H.; Sanchez, S.; Schmidt, O. G. *Nanoscale* **2012**, *5*, 1294−1297.
(62) Smith, E. J.; Xi, W.; Makarov, D.; Mönch, I.; Harazim, S.; Quiñones, V. A. B.; Schmidt, C. K.; Mei, Y.; Sanchez, S.; Schmidt, O. G. *Lab Chip* **2012**, *12*, 1917−1931.
(63) Soler, L.; Magdanz, V.; Fomin, V. M.; Sanchez, S.; Schmidt, O. G. *ACS Nano* **2013**, *7*, 9611−9620.
(64) Chalapat, K.; Chekurov, N.; Jiang, H.; Li, J.; Parviz, B.; Paraoanu, G. S. *Adv. Mater.* **2013**, *25*, 1.
(65) Bassik, N.; Brafman, A.; Zarafshar, A. M.; Jamal, M.; Luvsanjav, D.; Selaru, F. M.; Gracias, D. H. *J. Am. Chem. Soc.* **2010**, *132*, 16314−16317.
(66) Gultepe, E.; Randhawa, J. S.; Kadam, S.; Yamanaka, S.; Selaru, F. M.; Shin, E. J.; Kalloo, A. N.; Gracias, D. H. *Adv. Mater.* **2013**, *25*, 514−519.
(67) Gultepe, E.; Yamanaka, S.; Laflin, K. E.; Kadam, S.; Shim, Y.; Olaru, A. V.; Limketkai, B.; Khashab, M. A.; Kalloo, A. N.; Gracias, D. H.; Selaru, F. M. *Gastroenterology* **2013**, *144*, 691−693.
(68) Rimstidt, J. D.; Barnes, H. L. *Geochim. Cosmochim. Acta* **1980**, *44*, 1683−1699.
(69) Iler, R. K. *J. Colloid Interface Sci.* **1973**, *43*, 399−408.
(70) Hwang, S.-W.; Tao, H.; Kim, D.-H.; Cheng, H.; Song, J.-K.; Rill, E.; Brenckle, M. A.; Panilaitis, B.; Won, S. M.; Kim, Y.-S.; Song, Y. M.; Yu, K. J.; Ameen, A.; Li, R.; Su, Y.; Yang, M.; Kaplan, D. L.; Zakin, M. R.; Slepian, M. J.; Huang, Y.; Omenetto, F. G.; Rogers, J. A. *Science* **2012**, *337*, 1640−1644.
(71) Randhawa, J. S.; Leong, T. G.; Bassik, N.; Benson, B. R.; Jochmans, M. T.; Gracias, D. H. *J. Am. Chem. Soc.* **2008**, *130*, 17238−17239.
(72) Hill, A. E.; Hoffman, G. R. *Br. J. Appl. Phys.* **1967**, *18*, 13.
(73) Fang, M.; Hu, D.; Shao, J. *Chin. Opt. Lett.* **2010**, *8*, 119−122.
(74) Leplan, H.; Robic, J. Y.; Pauleau, Y. *J. Appl. Phys.* **1996**, *79*, 6926−6931.
(75) Nikishkov, G. P. *J. Appl. Phys.* **2003**, *94*, 5333−5336.
(76) Friede, B.; Jansen, M. *J. Non-Cryst. Solids* **1996**, *204*, 202−203.
(77) Schulmeister, K.; Mader, W. *J. Non-Cryst. Solids* **2003**, *320*, 143−150.
(78) Rui, L.; Cheng, H.; Su, Y.; Hwang, S.-W.; Yin, L.; Tao, H.; Brenckle, M. A.; Kim, D.-H.; Omenetto, F. G.; Rogers, J. A.; Huang, Y. *Adv. Funct. Mater.* **2013**, *23*, 3106−3114.
(79) Kang, S.-K.; Hwang, S.-W.; Cheng, H.; Yu, S.; Kim, B. H.; Kim, J.-H.; Huang, Y.; Rogers, J. A. *Adv. Funct. Mater.* **2014**, DOI: 10.1002/adfm.201304293.
(80) Pandey, S.; Ewing, M.; Kunas, A.; Nguyen, N.; Gracias, D. H.; Menon, G. *Proc. Natl. Acad. Sci. U.S.A.* **2011**, *108*, 19885−19890.
(81) Kummer, M. P.; Abbott, J. J.; Kratochvil, B. E.; Borer, R.; Sengul, A.; Nelson, B. J. *IEEE Trans. Robotics* **2010**, *26*, 1006−1017.